Shemin, D., & Russell, C. S. (1953) *J. Am. Chem. Soc. 75*, 4873–4874.
Smith, D. J., Maggio, E. T., & Kenyon, G. L. (1975) *Biochemistry 14*, 766–771.
Wilbur, D. J., Norton, R. S., Clouse, A. O., Addleman, R., & Allerhand, A. (1976) *J. Am. Chem. Soc. 98*, 8250–8254.
Windholz, M., Ed. (1976) *The Merck Index*, 9th ed., p 987, Merck, Rahway, NJ.

High-Resolution NMR Studies of Fibrinogen-like Peptides in Solution: Resonance Assignments and Conformational Analysis of Residues 1–23 of the Aα Chain of Human Fibrinogen†

Feng Ni and Harold A. Scheraga*
Baker Laboratory of Chemistry, Cornell University, Ithaca, New York 14853-1301
Susan T. Lord
Department of Pathology, University of North Carolina, Chapel Hill, North Carolina 27514
Received October 27, 1987; Revised Manuscript Received February 12, 1988

ABSTRACT: The proton resonances of the following synthetic linear human fibrinogen-like peptides were completely assigned with two-dimensional NMR techniques in solution: Ala(1)-Asp-Ser-Gly-Glu-Gly-Asp(7)-Phe-Leu-Ala-Glu-Gly(12)-Gly(13)-Gly(14)-Val(15)-Arg(16)-Gly-Pro-Arg-Val-Val-Glu-Arg (F10), Ala-Asp-Ser-Gly-Glu-Gly-Asp-Phe-Leu-Ala-Glu-Gly-Gly(13)-Gly(14)-Val-Arg (F11), and Gly-Pro-Arg-Val-Val-Glu-Arg (F12). No predominant structure was found in the chain segment from Ala(1) to Gly(6) for F10 in both H_2O and dimethyl sulfoxide. The previous suggestion that there is a hairpin loop involving residues Gly(12) to Val(15) in the Aα chain of human fibrinogen is supported by the slow backbone NH exchange rates of Gly(14) and Val(15), by an unusually small NH chemical shift of Val(15), and by strong sequential NOE's involving this region in F10. This local chain fold within residues Asp(7) to Val(20) may place the distant Phe residue near the Arg(16)–Gly(17) peptide bond which is cleaved by thrombin.

The specific removal of fibrinopeptides A and B by thrombin exposes complementary polymerization sites near the N-terminus of the Aα and Bβ chains (Laudano & Doolittle, 1980) located in the central domain of the soluble plasma protein fibrinogen (Telford et al., 1980), an event which initiates the spontaneous polymerization of the resultant fibrin monomer into the insoluble fibrin clot [Scheraga (1983, 1986) and references cited therein]. Much has been learned in recent years about the mechanism of the interaction of thrombin with fibrinogen, especially about the cleavage of the Arg–Gly peptide bond in the Aα chain of human fibrinogen [Scheraga (1983, 1986) and references cited therein]. Among other things, by use of an active-site mapping approach, one of the thrombin (catalytic) binding sites has been found to lie within the region from Asp(7) to Val(20) near the N-terminus of the human fibrinogen Aα chain [Meinwald et al., 1980; Marsh et al. (1983) and references cited therein]. In particular, residues Asp(7) and Phe(8), which are located ten and nine residues away, respectively, from the thrombin cleavage site, have been shown to influence the effectiveness of the binding of synthetic peptide substrates to thrombin (Marsh et al., 1982, 1983). These kinetic data help explain the observations that Asp(7) and Phe(8) are strongly conserved in many species (Blombäck, 1967; Henschen et al., 1983) and that mutations of Asp(7) to Asn(7) and Arg(19) to Asn(19) or Ser(19) produce bleeding disorders [Henschen et al., 1983; Menache (1983) and references cited therein].

In contrast to the understanding that has been gained about the influence of residues around the Arg–Gly peptide bond on the kinetics of cleavage of this bond, very little progress has been made to elucidate the detailed mechanism of the interaction of fibrinogen with thrombin, primarily because crystal structures of thrombin and fibrinogen are not available. With use of physicochemical techniques such as NMR[1] spectroscopy, attempts have been made to determine conformational features of small peptide substrates of thrombin in aqueous and in nonaqueous solutions such as DMSO (von Dreele et al., 1978; Rae & Scheraga, 1979). However, these studies were limited to very small peptides, whereas it is now clear that long-range interactions not present in those small

† This work was supported by research grants from the National Institute of General Medical Sciences (GM-24893) and the National Heart, Lung, and Blood Institute (HL-30616 and HL-31048), National Institutes of Health. It was carried out with the GN-500 500-MHz NMR spectrometer at the NIH Regional Research Resource for Multinuclear NMR and Data Processing at Syracuse University (RR-01317). This is paper 16 in a series. Marsh et al. (1985) is paper 15 of this series.
* Correspondence should be addressed to this author.

[1] Abbreviations: NMR, nuclear magnetic resonance; DMSO, dimethyl sulfoxide; NOE, nuclear Overhauser effect; HPLC, high-performance liquid chromatography; RPLC, reverse-phase HPLC; TFA, trifluoroacetic acid; PAM, phenylacetamidomethyl; Tos, tosyl; *t*-Boc, *tert*-butyloxycarbonyl; Bzl, benzyl; DCC, *N,N*-dicyclohexylcarbodiimide; HF, hydrofluoric acid; DMSO-d_6, fully deuteriated DMSO; EDTA, ethylenediaminetetraacetic acid; Tris, tris(hydroxymethyl)aminomethane; COSY, two-dimensional scalar correlation spectroscopy; DQ-COSY, double quantum filtered COSY; NOESY, two-dimensional nuclear Overhauser and exchange spectroscopy; relayed COSY, two-dimensional relayed *J*-correlation spectroscopy; FpA, fibrinopeptide A; FpAP, phosphorylated fibrinopeptide A; des-A fibrin, fibrin produced after only FpA and FpAP are removed from fibrinogen.

0006-2960/88/0427-4481$01.50/0

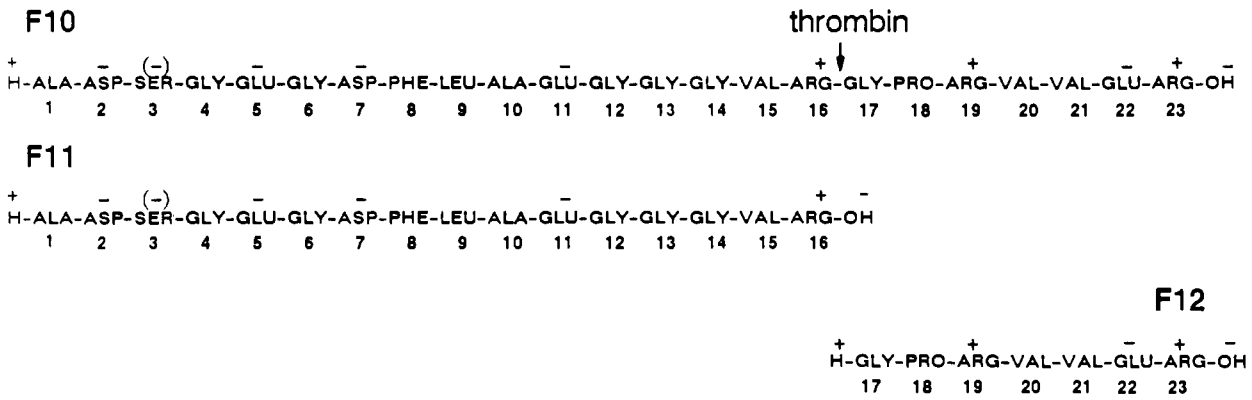

FIGURE 1: Amino acid sequences of peptide F10, F11, and F12. The numbering is that of the Aα chain of human fibrinogen, and the charges are those at neutral pH. The negative charge of Ser(3) is due to partial phosphorylation of this residue in native human fibrinogen.

peptides are necessary for adequate binding of native fibrinogen to thrombin (Nagy et al., 1982; Marsh et al., 1983; Hanna et al., 1984). Recently, an NMR study of the much larger peptide F8 [corresponding to Asp(7) to Val(20) of the Aα chain of human fibrinogen] was carried out in aqueous solution (Marsh et al., 1985). On the basis of that NMR study and previous kinetic and immunochemical data, it was suggested that a significant amount of β-bend might exist around Gly(12) to Val(15) in the larger peptide, F8, which could be stabilized by a possible salt link between Asp(7) and Arg(19). The absence of such a long-range interaction (thereby destabilizing the intervening β-bend) could account for the delayed release of fibrinopeptide A from both fibrinogen Lille and fibrinogen Munich in which Asp(7) is replaced by Asn(7) and Arg(19) by Asn(19), respectively (Morris et al., 1981; Henschen et al., 1981).

Under the hypothesis that a nativelike conformation can be stabilized in larger fragments of the native protein, as observed previously (Hogg & Blombäck, 1978), we have synthesized a peptide corresponding to residues Ala(1) to Arg(23) (Figure 1) of the Aα chain of human fibrinogen. It contains the sequences of all of the peptides studied previously (Meinwald et al, 1980; Marsh et al., 1983). We have carried out an NMR conformational analysis of this peptide and fragments thereof (Figure 1) using one- and two-dimensional NMR methods with which the proton NMR resonances of proteins containing up to 60 amino acid residues have been completely assigned and their solution structures determined (Wüthrich et al., 1982; Billeter et al., 1982; Wagner & Wüthrich, 1982; Wider et al., 1982; Wüthrich, 1986; Montelione et al., 1987). In our present study, we cannot hope to determine the three-dimensional structure of the isolated 23-residue linear peptide in aqueous solution because such a linear peptide generally exists as an ensemble of many conformational states of similar energy; i.e., it does not adopt a single native, low-energy form as it presumably does when connected to the whole fibrinogen molecule. We, however, present here the complete sequence-specific proton resonance assignments related to the linear peptide in solution and discuss the conformational features of the free peptides as derived from the NMR data. These assignments will form the basis for our ongoing efforts to determine the structure of this peptide in a complex with thrombin, by use of the transferred NOE technique (Clore & Gronenborn, 1982, 1983).

Experimental Procedures

Materials and Instrumentation. Fibrinogen (human, Kabi grade L) was a gift from Dr. G. Claeson, and atroxin (*Bothrops atrox* venom, Sigma) was a commercial product. Human α-thrombin was a gift from Dr. J. W. Fenton II (New York State Department of Health, Albany, NY).

Peptide purification and analysis were carried out on an SP 8000 liquid chromatograph (Spectra Physics) equipped with a computer-controlled solvent delivery system and a variable-wavelength light absorbance detector. The reverse-phase HPLC (RPLC) column was a Waters RadPak analytical C_{18} cartridge connected to the chromatography system with a Waters Radial Compression Module (RCM-100). Flow phase A was 0.09% aqueous trifluoroacetic acid (TFA) (pH 2.1), and flow phase B was 0.09% TFA in acetonitrile.

NMR experiments were carried out on a 500-MHz GN-500 series superconducting spectrometer (General Electric) located at the Syracuse NIH NMR Resource facility. The spectrometer was equipped with a Doric variable-temperature unit. NMR data from one-dimensional experiments were analyzed and plotted with the spectrometer computer. Two-dimensional data were transmitted to a Vax 8650 computer by the software developed at the Resource. Zero filling, digital filtering, and two-dimensional Fourier transformation of the free induction decays (FID's) were all performed with the NMR2 software system (Levy et al., 1986).

Synthesis of the Aα 1–23 Peptide. The Aα 1–23 peptide was synthesized by solid-phase methodology with an Applied Biosystems 420a automated peptide synthesizer. All reagents were obtained directly from Applied Biosystems, Inc. The starting resin was 0.8 g of phenylacetamidomethyl (PAM) resin (1% polystyrene cross-linked with divinylbenzene) loaded with 0.62 mmol/g arginine [*t*-Boc-L-Arg(Tos)]. All amino acids were L-α-amino *t*-Boc derivatives, and were used at a 4 M excess. In addition, glutamate and aspartate side chains were protected with *O*-Bzl, serine was protected with Bzl, and arginine was protected with Tos. At the beginning of each cycle, the *t*-Boc groups were removed with ~30% TFA. All residues were singly coupled with preformed symmetrical anhydrides of *N,N*-dicyclohexylcarbodiimide (DCC), except for arginine residues which were doubly coupled as active esters with 1-hydroxybenzotriazole and DCC. The coupling efficiency of each addition was determined by the quantitative ninhydrin procedure (Sarin et al., 1981).

The protecting groups were removed by HF cleavage. To 1.0 g of resin–peptide, 10.0 mL of HF, 1.0 mL of anisole, and 1.0 mL of dimethyl sulfide were added, and the reaction was maintained at −2.0 °C for 60 min. After rapid evaporation of the HF in a flowing stream of nitrogen, the resin was washed with diethyl ether to remove scavengers. The peptide was dissolved in 30% aqueous acetic acid and lyophilized. The

deprotection yielded 0.44 g of the crude peptide material.

Analysis of the Solid State Synthesized Peptide. A small fraction of the HF-treated material was dissolved in flow solvent A and applied to the RPLC column equilibrated with this same solvent. The peptide material was eluted from the column by a 58-min gradient run from 2% to 60% acetonitrile and detected at a wavelength of 205 nm. The main component (77%) had an amino acid composition of Asp(1.95,2), Glu(3.23,3), Ser(1.01,1), Gly(6.38,6), Arg(2.83,3), Ala(2.09,2), Pro(1.16,1), Val(2.47,3), Leu(0.89,1), and Phe(0.98,1).

Thrombin Cleavage of the Synthetic Peptide and Purification of Cleavage Products. A total of 80 mg of the crude peptide material was dissolved in a buffer that was 150 mM in NaCl and 50 mM in Tris. The pH of the peptide solution was adjusted to 7.6. The solution was incubated overnight at room temperature in the presence of 40 NIH units/mL of human thrombin. The pH of the solution was then adjusted to 2.0 with 1.0 M HCl to stop the thrombin action. The cleavage products were assayed and purified by the analytical RPLC procedure (see previous paragraph). Two main peaks were obtained during gradient elution. The early-eluted component had an amino acid composition of Glu(1.14,1), Gly(1.13,1), Arg(2.22,2), Pro(1.11,1), and Val(1.40,2) and the second Asp(1.91,2), Glu(2.17,2), Ser(0.90,1), Gly(5.26,5), Arg(1.10,1), Ala(2.02,2), Val(0.89,1), Leu(0.87,1), and Phe(0.95,1). Thus, they correspond to fragments 17–23 (F12) and 1–16 (F11), respectively.

Peptide Purification. Further purification of the crude peptide material F10 and its thrombin cleavage products was achieved by a preparative RPLC procedure. For this purpose, a Dynamax preparative C_{18} column was employed with the SP 8000 chromatograph using an isocratic flow phase of 80% flow solvent A and 20% flow solvent B (see an above section). The yield of the pure peptide was about 70% for an average run. All of the peptides exhibited a symmetric peak (>95%) in subsequent analytical RPLC runs. The purified peptides were lyophilized to fluffy powders to free them from residual TFA contained in the RPLC solvent.

NMR Sample Preparation and Measurements. Various peptides (10–20 mg/mL) were dissolved in 0.4 mL of either DMSO-d_6 (Cambridge Isotopes) or an aqueous solution that was 150 mM in NaCl, 50 mM in sodium phosphate, and 0.1% in NaN_3 at pH 5.3. All samples in H_2O contained 10% D_2O as the lock solvent. The pH values of the aqueous samples were checked regularly with an Ingold electrode without correction for the presence of D_2O. Samples in D_2O were prepared by lyophilizing the corresponding samples in H_2O; the lyophilized powder (peptide and salts) was then dissolved in 0.4 mL of 99.96% D_2O (Cambridge Isotopes). To eliminate possible interference from paramagnetic metal ions in NOE measurements, all of the NMR tubes were treated with a wash cycle of Nochromix (Godax) solution, 1 M EDTA, and distilled and deionized water. The solvent for NOE measurements in aqueous solutions also contained 0.2 mM EDTA as a metal scavenger. Samples were flushed with dry nitrogen before measurements whenever necessary.

One-dimensional proton spectra of the peptides in either DMSO or D_2O were acquired with a simple one-pulse sequence $(90\text{–}t_2\text{–}t_d)_n$ incorporating the CYCLOPS phase cycling of the radio-frequency pulse for the suppression of quadrature images (Hoult & Richards, 1975). The postacquisition delay, t_d, was set to 2 s to ensure an equilibrium condition before the next pulse. Spectra in H_2O solutions were obtained with the jump–return pulse (Plateau & Gueron, 1982). One-dimensional spectra of F10 were recorded in the concentration range of 1 mg/mL (~0.5 mM) to 40 mg/mL (~20 mM). No significant line broadening was observed at higher concentrations compared to lower concentration; this suggests that aggregation of the peptides was minimal under the experimental conditions.

Two-Dimensional NMR Spectroscopy. For spectra in D_2O and DMSO, J correlation of the proton resonances (COSY) was acquired with the sequence $(90\text{–}t_1\text{–}90\text{–}90\text{–}t_2\text{–}t_d)_n$ with appropriate phase cycling to achieve double-quantum filtration for diagonal suppression in the resulting spectra (DQ-COSY; Piantini et al., 1982; Shaka & Freeman, 1983). Two-dimensional nuclear Overhauser and exchange spectra (NOESY) were obtained with the sequence $(90\text{–}t_1\text{–}90\text{–}t_m\text{–}90\text{–}t_2\text{–}t_d)_n$ with phase cycling to suppress J cross-peaks except for those due to zero-quantum coherence transfer (Jeener et al., 1979; Macura et al., 1981). Relayed J-correlation spectra (relayed COSY; Bolton & Bodenhausen, 1982; Eich et al., 1982; King & Wright, 1983; Wagner, 1983) were obtained with the sequence $(90\text{–}t_1\text{–}90\text{–}t_m\text{–}180\text{–}t_m\text{–}90\text{–}t_2\text{–}t_d)_n$ with t_m set to 16 ms and with appropriate phase cycling to suppress spectrometer artifacts (Bax & Drobny, 1985). All COSY spectra were averages of 16 or 32 transients with a small t_d (typically 800 ms). A total of 256 FID's of 1K complex data points were acquired and transformed into magnitude spectra (Aue et al., 1976) of size 1K × 1K with a nonshifted sine bell multiplication in both the t_1 and t_2 directions before Fourier transformation (Wider et al., 1984). NOESY spectra were results of 32 transients with relatively long t_d (about 1.5 s). A total of 256 FID's of 1K complex data points were acquired with the double block acquisition procedure (States et al., 1982). The FID matrices were all premultiplied by the square of a 54° shifted sine bell in both the t_1 and t_2 directions. The pure-phase (Aue et al., 1976) spectra of size 1K × 1K were then calculated from the FID matrices by a hypercomplex two-dimensional Fourier transformation (States et al., 1982) and phased in the f_2 direction to pure absorption with phase parameters obtained from the first slice of the FID matrix (corresponding to zero t_1). Phase adjustments in the f_1 direction were minimal and only zeroth order (typically 10°) for the Bessel filter setting of the receiver.

COSY spectra in H_2O were obtained by inserting the jump–return into the sequence $(90\text{–}t_1\text{–}90\text{–}t_2\text{–}t_d)_n$ in a similar way as described elsewhere for other solvent-suppression techniques (Hore, 1983, 1984). DQ-COSY spectra were acquired with the sequence for ZZ coherence transfer, $(90\text{–}t_1\text{–}45\text{–}t_m\text{–}45\text{–}t_2\text{–}t_d)_n$ (Bodenhausen et al., 1984), with the incorporation of a short z_1 gradient pulse at the beginning of t_m and replacement of the last 45° pulse by a selective excitation pulse similar to a procedure described elsewhere (Zuiderweg, 1987). The length of the z_1 gradient and the time delay t_m (time of homospoil recovery) were optimized for good water suppression and a high signal-to-noise ratio of the acquired FID's. Relayed COSY spectra in H_2O were acquired with the same sequence described above for D_2O and DMSO samples except that a selective water saturation pulse was turned on at both the t_d and t_m time periods. NOESY spectra were acquired with a short z_1 gradient pulse at the beginning of the t_m mixing period to help suppress undesired J-coherence transfers (Macura et al., 1981). This homospoil pulse also served to eliminate any residual water signal in the transverse plane due to imperfections of the 90° pulses (Basus, 1984). To avoid excitation of the large water signal, the last 90° pulse was replaced by the jump–return pulse. The length of the z_1 gradient was set to the same value as that in the ZZ DQ-COSY sequence. Acquisition and processing of the FID's were

the same as for the D_2O and DMSO samples.

Temperature Dependence of Amide Proton Chemical Shift. Solutions of F10 and F11 at 20 mg/mL (~10 mM) and pH 5.3 were used to obtain data on the temperature dependence of the chemical shifts of the amide protons in one-dimensional spectra of the peptides in H_2O. Temperatures represent the nominal values on the variable-temperature control unit. At all temperatures in the range of 12–42 °C, chemical shifts were referenced with respect to the most upfield doublet of the $C^{\delta}H$ of Leu(9) calibrated to be 0.86 ppm by use of the HOD proton resonance of 4.80 ppm at 298 K at pH 5.3. Temperature coefficients of the amide chemical shifts were estimated from curves for chemical shift vs temperature for all resolvable amide resonances in the range of 12–42 °C.

Qualitative NH Proton Exchange Spectroscopy. The relative rates of exchange of amide protons were determined by qualitatively following the kinetics of proton–deuterium exchange. Usually, the peptide or protein is first lyophilized from H_2O. Immediately after the lyophilized sample is dissolved in pure D_2O, the residual NH signal intensities are followed with time. The relative rates of decay of various NH signals will be a measure of exchange rates of NH protons with deuterium of different amino acid residues. This simple procedure cannot be applied directly in our study because the intrinsic lifetimes of NH protons in small peptides are in general on the order of a few seconds to a few minutes (Molday et al., 1972). We, therefore, adopted a simple temperature jump procedure in which the peptide was dissolved in D_2O under the desired conditions for a given length of time (room temperature at pH 3.0). Then, the NMR tube containing the peptide was immediately lowered into the probe where the temperature had been preequilibrated to 0 °C, a condition under which the exchange lifetime is increased to a few hundred minutes for exchanging protons in a nonstructured peptide (Englander & Poulsen, 1969). The resonances of the *trapped* NH protons were then assigned, and the intensities were analyzed as a function of the time lag between the dissolution and the start of spectral acquisition. The ambiguities due to overlapping NH peaks were removed by recording a COSY spectrum of the trapped NH protons in D_2O at 0 °C and pH 3.0.

The relative exchange rates of NH protons in F10 were further confirmed qualitatively by solvent saturation transfer (Campbell et al., 1977), two-dimensional exchange spectroscopy (Jeener et al., 1979) of peptide NH and solvent protons (Dobson et al., 1986), and pH dependence of NH resonance line shapes (Takeda & Stejskal, 1960). In solvent saturation transfer experiments, the water proton signal was selectively irradiated for 1 s before the observation of peptide NH proton signals in H_2O by the jump–return sequence. Fast-exchanging NH protons (lifetime less than 500 ms) can readily be identified because they will be selectively attenuated or eliminated due to magnetization transfer. For exchanging protons with lifetimes on the order of or longer than the T_2's, the magnitudes of the exchange cross-peaks in a NOESY spectrum of 500-ms mixing time were used to compare relative exchange rates (Dobson et al., 1986). The coalescence of NH doublets upon increasing the pH was also used to resolve further ambiguities (Takeda & Stejskal, 1960).

Binding Experiments of Thrombin Cleavage Products of F10. To determine whether F11 binds to F12, we followed the proton NMR binding experiment reported by Root-Bernstein and Westall (1984). For this purpose, stock solutions of F11 and F12 were prepared at ~15 mg/mL in a 50 mM sodium phosphate buffer that was 150 mM in NaCl, with the pH adjusted to 6.0. The solution of F11 and F12 was then diluted with the same buffer to make up three samples of the mixtures of F11 and F12 at volume ratios of 6:1, 3:1, and 3:2 (mole ratios of 6:1, 3:2, and 1:1, respectively) of the stock solutions. After being incubated for about 1 h at room temperature, the pH's of the samples were checked and adjusted to the desired values. The proton NMR spectra were then taken of all the samples at both pH 6.0 and pH 7.0.

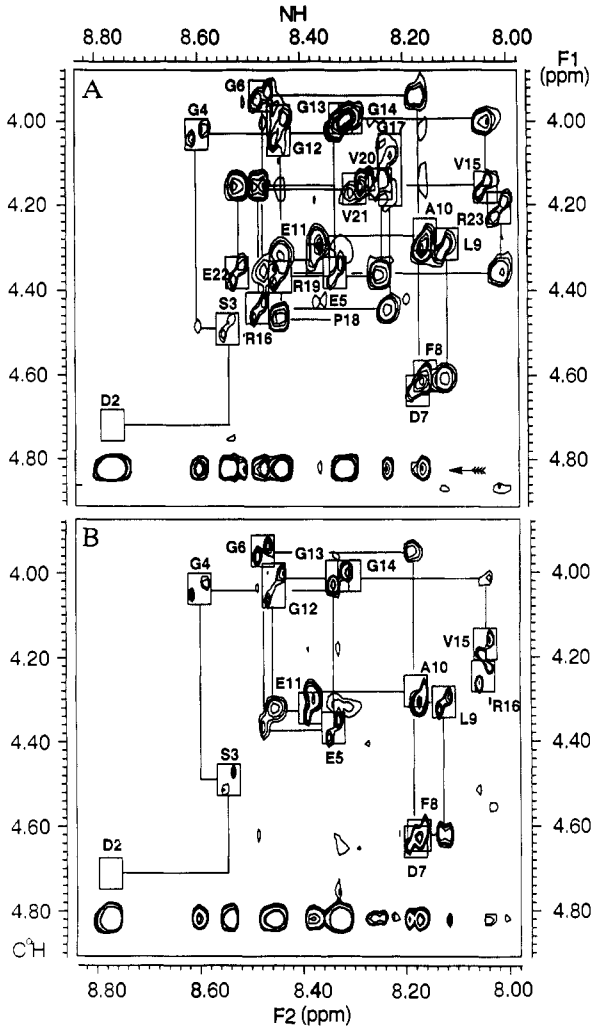

FIGURE 2: (A) NOE map of the $C^{\alpha}H$ and NH resonances of F10 (with t_m = 500 ms) in H_2O at pH 5.3 and 25 °C. Specific intraresidue $C^{\alpha}H$–NH interactions are labeled by the corresponding amino acid residues. The sequential $C^{\alpha}H$–NH NOE cross-peaks are connected by lines going from Arg(23) to Pro(18) and from Gly(17) to Asp(2). The intraresidue $C^{\alpha}H$–NH NOE and interresidue $C^{\alpha}H$–NH NOE between Asp(2) and Ser(3) are not detected because of the fast exchange of the NH protons of both Asp(2) and Ser(3). The cross-peaks at 4.82 ppm (arrow) appear because of chemical exchange of the NH protons in the peptide with protons of the aqueous solvent. (B) The sequential NOE connectivities of the natural F11 (FpA) (with t_m = 500 ms) in H_2O at pH 5.3 and 25 °C.

RESULTS

Confirmation of the Amino Acid Sequence of the Synthetic F10. First, the assignments of resonances to specific amino acid types were established by use of the *J*-connectivity patterns of different spin systems in the COSY (Kessler & Bermel, 1986; Wüthrich, 1986) and relayed COSY spectrum (Wagner, 1983; Wüthrich, 1986). The backbone NH proton of Arg(23) was identified as the most upfield shifted of the NH's of all the arginines because of its terminal location (Figure 2A). The sequence in the region of Pro(18)–Arg(23) was confirmed by analysis of the sequential $C^{\alpha}H$–NH NOE

connectivities starting from Arg(23) (Figure 2A). The tracing from Arg(23) to Pro(18) is unambiguous. The appearance of strong NOE cross-peaks (spectra not shown) between the $C^{\delta}H$ of Pro(18) and a signal corresponding to the $C^{\alpha}H$ of one of the glycines confirmed that position 17 is occupied by a glycine. The existence of those NOE's also demonstrates that Pro(18) assumes a trans conformation in F10 in H_2O (see later sections).

The sequence of region Ala(1) to Arg(16) cannot be checked unambiguously by use of the NOESY spectrum of F10 alone. We, therefore, recorded a NOESY spectrum of the natural FpA purified from the supernatant of the des-A fibrin clot. The NOE connectivity map of FpA is shown in Figure 2B. Again, Arg(16) shows an upfield shift from 8.48 to 8.04 ppm as a result of thrombin cleavage [Arg(16) is now at the terminal location]. Starting from this residue, we see that the NOE pattern matches the rest of the NOE connectivities in Figure 2A. We are, thus, certain that the synthetic F10 has the correct sequence from the combination of the results of amino acid compositions (see Experimental Procedures) of thrombin cleavage products of F10 and the two-dimensional $C^{\alpha}H$ and NH NOE cross-peak patterns.

Sequence-Specific Resonance Assignments. After the amino acid sequences of the peptides were established, residue-specific assignments for NH and $C^{\alpha}H$ protons in F10 and F11 were carried out by use of the sequential-assignment technique (Wüthrich et al., 1982; Wüthrich, 1986). The locations of most of the protons of the aliphatic side chains were further established by the combination of relayed COSY and NOESY spectra at long mixing times (500 ms). The NH resonances of Gly(13) and Gly(14) in both F10 and F11 partially overlap with the NH resonances of Glu(5), Gly(17), Val(20), and Val(21). In two dimensions, they are well separated from the cross-peaks of Glu(5), Gly(17), Val(20), and Val(21), as seen in Figure 2A. Further resolution, and hence assignment, of the partially overlapped NH–$C^{\alpha}H$ cross-peaks such as those of Gly(13) and Gly(14) was facilitated by comparison with spectra of small peptide fragments [Phe(8)–Pro(18)] specifically deuteriated at $C^{\alpha}H$ of Gly(13) and Gly(14) (Marsh et al., 1985). For peptide F12, specific resonance assignments were made by analyzing its COSY spectra in H_2O and by comparing the NH–$C^{\alpha}H$ J correlations with those of peptide F10.

Proton Chemical Shifts in H_2O and DMSO. In Table I, the chemical shifts of the proton resonances of F10 are compared with those of F11 and F12 at 25 °C. Table II lists the chemical shifts of F10 in DMSO at 25 °C. Tables I and II also contain the deviations from reference values of the chemical shifts of nonstructured peptides (Bundi et al., 1975; Bundi & Wüthrich, 1979; Wüthrich, 1986) for comparison. All chemical shifts were estimated from NOESY maps of the peptides under similar solvent conditions as the samples used for one-dimensional variable-temperature measurements. Because of the limited resolution of the two-dimensional spectra, the numerical values are accurate only to within ±0.01 ppm.

From Table I, it is seen that there are significant deviations of the backbone amide proton chemical shifts from reference values for residues from Asp(2) to Gly(4), Asp(7), Leu(9), and Val(15) to Arg(23) for F10, F11, and F12 in H_2O. For Asp(2), Ser(3), and Gly(4), the deviations can be attributed to the influence of the positive charge of the free terminal amino group, $^{+}H_3N$–. In fact, this group is also the cause of the large exchange rate of the NH of Asp(2), as discussed in later sections. The ring current of Phe(8) causes the deviations

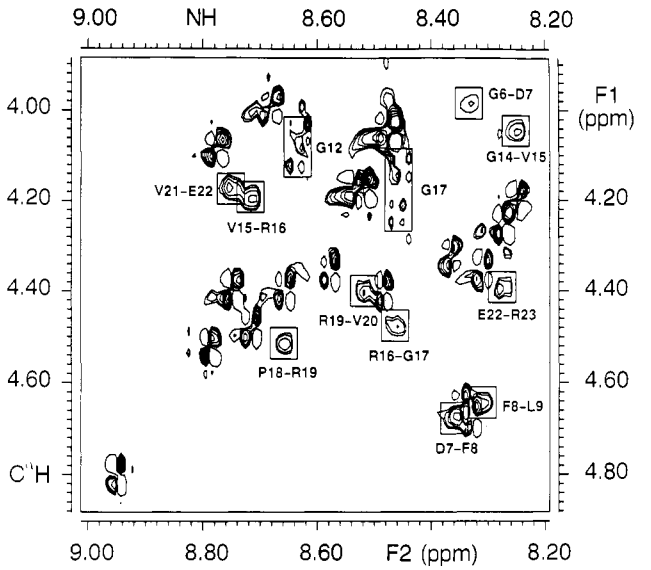

FIGURE 3: The $C^{\alpha}H$–NH region of the NOESY spectrum of F10 in H_2O at 0 °C, with a 30-ms mixing time (t_m). Interresidue NOE's are indicated by the amino acid residues involved. The two sets of cross-peaks labeled as G12 and G17 result from intraresidue $C^{\alpha}H$–NH zero quantum coherence transfer. They indicate that both Gly(12) and Gly(17) have nondegenerate geminal $C^{\alpha}H$ protons as compared to other glycines in the sequence (see Figure 2A).

of residues Asp(7) and Leu(9). This follows from the fact that the NH chemical shifts of Phe(8) are not significantly different from the reference shift. The NH proton with the largest deviation (−0.38 ppm) from the reference shift is that of Val(15). It is seen that this trend of large deviations propagates through the carboxyl-terminal residue, Arg(23). It is also interesting to note that the NH proton of Gly(12) is well resolved from all the five other glycines along the peptide backbone and especially from its neighbor glycines, Gly(13) and Gly(14). Furthermore, the geminal $C^{\alpha}H$ protons of Gly(12) are resolved from each other in a very similar way as the splitting of $C^{\alpha}H$ geminal protons of Gly(17) which is near a conformationally restricted residue, Pro(18). This phenomenon can be seen clearly from the pattern of cross-peaks arising from intraresidue NH–$C^{\alpha}H$ NOE's in both Figure 2A and Figure 3.

The backbone NH chemical shifts of various residues remain largely unchanged after thrombin cleavage of the Arg(16)–Gly(17) peptide bond. The exceptions are Arg(16), Arg(19), and Val(20). As mentioned before for Arg(23), the terminal location of Arg(16) in F11 is the cause of its abnormal NH chemical shift. In fact, Arg(23) remains upfield shifted in F12. With Arg(19) and Val(20), the most obvious explanation for the changes of chemical shifts from those in intact F10 is the influence of the free N-terminal amino group in F12.

The backbone NH chemical shifts of peptide F10 show a concerted trend to larger values as the temperature is decreased from 42 °C down to −8 °C. The $C^{\alpha}H$ and aliphatic CH's, on the other hand, remain unchanged throughout the temperature range studied.

The chemical shifts of the NH's of Asp(7) and Leu(9) approach those of nonstructured peptides in DMSO solutions (Bundi et al., 1975). On the other hand, the NH of Phe(8) is shifted away from the reference. In the region of residues Val(15) to Arg(23), the NH's of Val(15) and Arg(16) are not different from those of nonstructured peptides whereas, from Gly(17) to Arg(23), the NH chemical shifts remain largely shifted in agreement with observations in H_2O. Again, the large downfield shift of the Asp(2) NH is due to the presence of the positively charged $^{+}H_3N$– at the N-terminus.

Table I: ^{1}H NMR Chemical Shifts (in ppm) of F10, F11, and F12 in H_2O at pH 5.3 and 25 °C

amino acid residue	NH			$C^\alpha H$			$C^\beta H$			other	
	F10	F11 and F12	F10 − NSP[a]	F10	F11 and F12	F10 − NSP[a]	F10	F11 and F12	F10 − NSP[a]	F10	F11 and F12
A1				4.20	4.20	0.15	1.55	1.55	0.15		
D2	8.77	8.77	0.36	4.71	4.70	0.05	2.76	2.76	−0.08		
		8.84[b]					2.66	2.66	−0.05		
S3	8.55	8.54	0.17	4.49	4.46	0.01	3.92	3.92	0.03		
							3.99	3.99	0.10		
G4	8.60	8.60	0.21	4.02	4.00	0.05					
E5	8.33	8.33	−0.04	4.36	4.34	0.07	2.01	2.00	0.04	2.31 ($C^\gamma H$)	2.30 ($C^\gamma H$)
							2.09	2.10	0.00		
G6	8.48	8.47	0.09	3.94	3.92	−0.03					
D7	8.19	8.17	−0.22	4.64	4.61	−0.12	2.66	2.64	−0.18		
							2.56	2.54	−0.19		
F8	8.17	8.16	−0.06	4.60	4.60	−0.06	3.20	3.15	−0.02	7.26 (o, PhH)	7.26 (o, PhH)
							3.09	3.06	0.10	7.37 (m, PhH)	7.37 (m, PhH)
										7.33 (p, PhH)	7.33 (p, PhH)
L9[c]	8.13	8.11	−0.29	4.31	4.30	−0.07	1.62	1.59	−0.03	0.86 ($C^\delta H$)	0.86 ($C^\delta H$)
							1.53	1.51	−0.12	0.93 ($C^\delta H$)	0.91 ($C^\delta H$)
A10	8.16	8.16	−0.09	4.29	4.26	−0.06	1.43	1.41	0.04		
E11	8.37	8.34	0.00	4.31	4.30	0.02	2.02	2.13	0.05	2.33 ($C^\gamma H$)	2.30 ($C^\gamma H$)
							2.10	1.98	0.01		
G12	8.45	8.45	0.06	4.07	4.04	0.10					
				3.99	3.97	0.02					
G13	8.34	8.33	−0.05	4.01	4.01	0.04					
G14	8.30	8.30	−0.09	3.99	4.00	0.02					
V15	8.06	8.04	−0.38	4.15	4.15	0.03	2.10	2.03	−0.03	0.95 ($C^\gamma H$)	0.95 ($C^\gamma H$)
										0.98 ($C^\gamma H$)	0.96 ($C^\gamma H$)
R16	8.48	8.05	0.21	4.44	4.22	0.04	1.81	2.11	0.01	1.67 ($C^\gamma H$)	1.64 ($C^\gamma H$)
							1.91		0.00	3.22 ($C^\delta H$)	3.21 ($C^\delta H$)
										6.72 (GuNH)	6.72 (GuNH)
										7.23 (ωNH)	7.23 (ωNH)
G17	8.24		−0.15	4.08	4.06	0.11					
				4.19		0.22					
P18				4.46		0.02	2.31	2.34	0.03	2.04 ($C^\gamma H$)	2.08 ($C^\gamma H$)
							1.92		−0.10	3.66 ($C^\delta H$)	3.60 ($C^\delta H$)
R19	8.45	8.55	0.18	4.36	4.32	−0.04	1.86	1.83	−0.05	1.67 ($C^\gamma H$)	1.64 ($C^\gamma H$)
							1.80		0.00	3.22 ($C^\delta H$)	3.21 ($C^\delta H$)
										6.72 (GuNH)	6.72 (GuNH)
										7.23 (ωNH)	7.23 (ωNH)
V20	8.26	8.29	−0.18	4.15	4.13	−0.03	2.06	2.05	−0.07	0.95 ($C^\gamma H$)	0.93 ($C^\gamma H$)
										0.98 ($C^\gamma H$)	
V21	8.30	8.33	−0.14	4.15	4.13	−0.03	2.06	2.05	−0.07	0.95 ($C^\gamma H$)	0.93 ($C^\gamma H$)
										0.98 ($C^\gamma H$)	
E22	8.53	8.53	0.16	4.36	4.36	0.07	2.07	1.97	−0.02	2.32 ($C^\gamma H$)	
							1.95		−0.02		
R23	8.03	8.00	−0.24	4.21	4.19	−0.19	1.81	1.83	0.02	1.67 ($C^\gamma H$)	1.64 ($C^\gamma H$)
							1.91		0.00	3.22 ($C^\delta H$)	3.21 ($C^\delta H$)
										6.72 (GuNH)	
										7.23 (ωNH)	

[a] Deviations from values of nonstructured peptides in H_2O (Bundi & Wüthrich, 1979). [b] NH resonance currently assigned to NH of D2 of FpA with S3 phosphorylated. [c] $C^\gamma H$ resonances of Leu(9) are not resolved.

Proline Cis/Trans Equilibrium in H_2O and DMSO. In H_2O, the major population of Pro(18) is trans since there exist strong NOE's between the $C^\alpha H$'s of Gly(17) and the $C^\delta H$'s of Pro(18), indicating that those protons are less than 4 Å apart (Wüthrich et al., 1984; Wüthrich, 1986). In DMSO, strong NOE's are observed between the $C^\alpha H$'s of the larger population of Gly(17) and the $C^\delta H$ of Pro(18). For the smaller population of Gly(17), the NOE's are between the $C^\alpha H$'s of Gly(17) and the $C^\alpha H$ of Pro(18), which suggests that the Gly(17)–Pro(18) peptide group assumes a cis form (Wüthrich et al., 1984; Wüthrich, 1986). From the relative intensities of the two populations of Gly(17), we estimate that the cis/trans ratio increases to 30:70 in DMSO. It is interesting to note that this ratio is similar in F10 compared to those in the smaller peptides in both H_2O and DMSO (von Dreele et al., 1978).

In previous studies of smaller fibrinogen-like peptides, peak doubling was observed both for the residue preceding the proline and for the one after (Ala instead of Arg; von Dreele et al., 1978). In the present study, peak doubling propagates through residues Val(15) and Val(21) which are three residues away from Pro(18) (Table II). We have tentatively assigned the downfield-shifted NH of Val(15), the upfield-shifted NH of Gly(17), the downfield-shifted NH of Arg(19), and the upfield-shifted NH of Val(20) as those belonging to the ensemble of conformations containing a cis Gly(17)–Pro(18) peptide bond. This is based on the previous observation that the minor population of resonance-doubled residues belongs to the cis ensemble of Pro(18) (von Dreele et al., 1978). It is seen from Table II that the NH chemical shifts of the trans populations of Arg(19) and Val(20) exhibit shifts of their NH's and $C^\alpha H$'s compared to those of reference peptides. In fact, the exchange rates of the NH's of Arg(19) and Val(20) were observed to be relatively small for F10 in H_2O (see later sections), suggesting that there might be intramolecular hydrogen bonds involving these two residues.

Temperature Dependence of NH Chemical Shifts. The backbone NH chemical shifts of peptides F10 and F11 show a linear dependence on temperature from 42 °C down to −8 °C. Except for Gly(13) and Gly(14), the temperature coef-

Table II: ^{1}H NMR Chemical Shifts (in ppm) of F10 in DMSO at 25 °C

	NH		$C^\alpha H$		$C^\beta H$		
amino acid residue	F10	F10 − NSP[a]	F10	F10 − NSP[a]	F10	F10 − NSP[a]	other, F10
A1			3.82	−0.52	1.34	−0.12	
D2	8.68	0.47	4.65	0.02	2.57	−0.13	
S3	7.94	−0.04	4.23	−0.11	3.52	−0.08	
					3.61	0.01	
G4	*b*		3.74	−0.02			
E5	7.94	−0.11	4.28	−0.06	1.74	−0.13	2.24 ($C^\gamma H$)
					1.90	0.03	
G6	*b*		3.74	−0.02			
D7	8.13	0.08	4.55	−0.08	2.39	−0.05	
					2.62	−0.08	
F8	7.89	−0.25	4.44	−0.12	2.77	0.02	7.20 (PhH)
					2.79	−0.24	
L9[c]	7.97	0.02	4.28	−0.09	1.43		0.81 ($C^\delta H$)
A10	8.04	0.00	4.27	−0.07	1.19	−0.03	
E11	7.90	−0.15	4.28	−0.06	1.74	−0.13	2.24 ($C^\gamma H$)
					1.90	0.03	
G12	8.13	0.02	3.64	−0.12			
			3.73	−0.03			
G13	*b*		3.75	−0.01			
G14	*b*		3.75	−0.01			
V15	7.85 (trans)	−0.03	4.19 (trans)	−0.07	1.94	−0.03	0.81 ($C^\gamma H$)
	7.94 (cis)	0.06	4.14 (cis)	−0.12			
R16	8.13 (trans)	0.06	4.33 (trans)	−0.02	1.50	−0.06	1.46 ($C^\gamma H$)
	8.18 (cis)	0.11	4.30 (cis)	−0.05	1.67	0.11	3.10 ($C^\delta H$)
							7.50 (ωNH)
G17	7.88 (cis)	−0.27	3.97	0.21			
			3.84	0.08			
	7.96 (trans)	−0.19	3.84	0.08			
			3.52	−0.24			
P18[d]					2.18 (cis)		
			4.48 (cis)		1.93 (cis)		1.84 ($C^\gamma H$)
			4.35 (trans)		2.00 (trans)		
					1.84 (trans)		3.37 ($C^\delta H$)
R19	8.38 (cis)	0.29	4.32 (cis)	−0.06	1.59	0.03	1.46 ($C^\gamma H$)
	8.16 (trans)	0.10	4.28 (trans)	−0.10	1.67	0.08	3.10 ($C^\delta H$)
							7.50 (ωNH)
V20	7.78 (trans)	−0.10	4.22 (cis)	−0.04	1.92	−0.05	0.81 ($C^\gamma H$)
	7.93 (cis)	0.05	4.14 (trans)	−0.12			
V21	7.61	−0.27	4.14 (trans)	−0.12	1.92	−0.05	0.81 ($C^\gamma H$)
			4.20 (cis)	−0.02			
E22	7.95	−0.10	4.29	−0.05	1.74	−0.13	2.24 ($C^\gamma H$)
					1.90	0.03	
R23	8.19	0.12	4.14	−0.24	1.50	−0.06	1.46 ($C^\gamma H$)
					1.67	0.11	3.10 ($C^\delta H$)
							7.50 (ωNH)

[a] Deviations from values of nonstructured peptides in DMSO (Bundi et al., 1975). [b] Chemical shifts are in the range of 8.08–8.18 ppm. Specific assignments are not possible because of overlap of resonances. [c] $C^\gamma H$ resonances of Leu(9) are not resolved. [d] Reference chemical shifts for proline are not available in the literature.

ficients for both F10 and F11 fall in the range of −6.0 to −8.3 ppb/deg typically expected for solvent-exposed NH's, as in the smaller fibrinogen-like peptides studied previously (Marsh et al., 1985). The temperature coefficients of the NH chemical shifts of Gly(13) and Gly(14) were found to be −5.0 ppb/deg in F10 and −5.6 ppb/deg in F11, demonstrably smaller than those for the other NH's, a phenomenon found to exist for the corresponding residues in peptide fragments Phe(8) to Pro(18) (F6) and Asp(7) to Val(20) (F8) (Marsh et al., 1985).

NH–$C^\alpha H$ Coupling Constants. The NH–$C^\alpha H$ coupling constants were estimated from one-dimensional spectra. They were found to fall in the range of 6.5–8.0 Hz at 25 °C for F10, F11, and F12. No structural significance can be attributed to this observation since, for small peptides with fluctuating structures, the three-bond J couplings are always averaged to 7.5 Hz (Bundi & Wüthrich, 1979; Kessler & Bermel, 1986). At low temperatures, the coupling constants could not be determined accurately because of line broadening from increased viscosity of the solvent with decreasing temperature.

NH Proton Exchange Rate. In Figure 4, we present the COSY map of $C^\alpha H$ with residual NH resonances trapped at low temperature (0 °C) after F10 was dissolved in D_2O at room temperature for approximately 5 min. The peak assignments were established by comparison with the sequential NH–$C^\alpha H$ NOE map of F10 in H_2O at the same pH and salt concentration. From the COSY contour map, we see that Leu(9), Val(15), Arg(16), Arg(19), Val(20), and Arg(23) have relatively large cross-peaks and Phe(8), Ala(10), Glu(11), Gly(14), and Gly(17) have small cross-peaks. There are no cross-peaks for the other residues. Qualitatively, the residues with larger COSY cross-peaks can be attributed to slower exchanging NH protons of the corresponding residues. Thus, Leu(9), Val(15), Arg(16), Arg(19), Val(20), and Arg(23) have the slowest of all slowly exchanging protons. This conclusion was confirmed by analysis of the exchange cross-peaks indicated in Figure 2A, by solvent saturation transfer experiments, and by the pH dependence of the line shape of NH protons.

Sequential NOE's at Short Mixing Times. With a very short mixing time (30 ms), only relatively strong sequential $C^\alpha H$–NH NOE's were observable for F10 at 0 °C. These are presented in Figure 3. Among the strong $C^\alpha H$–NH NOE's

Table III: Summary of NMR Parameters for F10 in both H_2O and DMSO[a]

	1	2	3	4	5	6	7	8	9	10	11	12	13	14	15	16	17	18	19	20	21	22	23
	A	D	S	G	E	G	D	F	L	A	E	G	G	G	V	R	G	P	R	V	V	E	R
k_{ex}								A	B	A	A			A	B	B	A	X	B	B			B
$d_{\alpha N}$						A	A	A					?	B	B	B	B*	B	B	?	B	B	
d_{NN}						A	?	?	?	A	?		?	B	B	B	X	X		?		B	
T													A	A									
s(H_2O)		B	A	A			B		B						B	A	A		A	A	A	A	B
s(DMS)		B			A			B			A						A		A	A	B	A	A

[a] X, not expected from the amino acid sequence. ?, not resolved. k_{ex}, exchange rate of NH protons (B, very slow; A, slow). $d_{\alpha N}$, sequential $C^{\alpha}H(i)$–NH ($i + 1$) NOE's (B, strong; A, weak). d_{NN}, sequential NH(i)–NH ($i + 1$) NOE's (B, strong; A, weak). T, abnormal temperature dependence of NH chemical shift. $s(H_2O)$, residues with deviations of NH chemical shifts from nonstructured peptides in H_2O [B, very large ($\geq \pm 0.22$); A, large ($< \pm 0.22$; $> \pm 0.09$)]. s(DMS), residues with deviations of NH chemical shifts from nonstructured peptides in DMSO [B, very large ($\geq \pm 0.22$); A, large ($< \pm 0.22$; $> \pm 0.09$)]; these designations pertain only to resonances corresponding to the trans population of Pro(18) (see Table II). The asterisk (*) indicates that NOE's are between $C^{\alpha}H$'s of Gly(17) and $C^{\beta}H$'s of Pro(18).

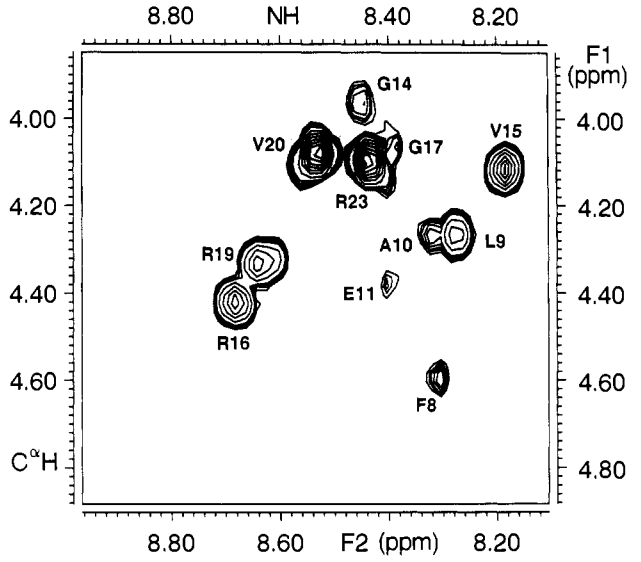

FIGURE 4: J correlation of residual NH protons with $C^{\alpha}H$ protons of F10 in D_2O at pH 3.0 and 0 °C. Lyophilized peptide and salts from a pH 3.0 sample were dissolved in D_2O for 5 min at room temperature. Spectral acquisition was started after the sample was equilibrated to 0 °C in the probe. A total of 256 FID's of 512 complex data points were acquired and processed with nonshifted sine bell multiplication in both dimensions. Final spectral size is 512 × 512.

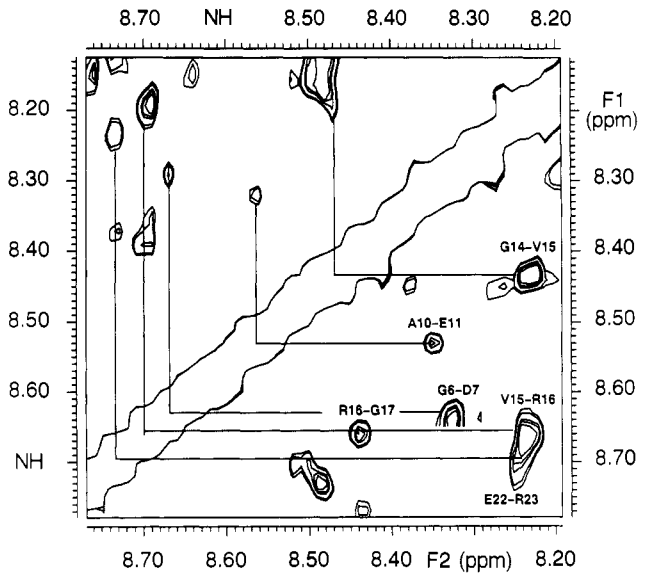

FIGURE 5: NH–NH region of the NOESY spectrum of F10 in H_2O at 5 °C, with a 100-ms mixing time. Interresidue NOE's are indicated by the amino acid residues involved.

are those between Gly(14) and Val(15), Val(15) and Arg(16), Arg(16) and Gly(17), Pro(18) and Arg(19), Arg(19) and Val(20), Val(21) and Glu(22), and Glu(22) and Arg(23). There are observable small NOE cross-peaks between Gly(6) and Asp(7), Asp(7) and Phe(8), and Phe(8) and Leu(9). Because of overlap of resonances, the possible existence of sequential NOE's between Gly(13) and Gly(14) and between Val(20) and Val(21) cannot be confirmed unambiguously. It is, however, clear that there are no observable sequential NOE's in the region from Ala(1) to Gly(6) and from Leu(9) to Gly(13) at this small mixing time.

The NH–NH NOE's of F10 in Figure 5 were recorded with a mixing time of 100 ms at 5 °C. The assignments of some of the very weak NOE's were established by comparison with the NH–NH NOE connectivities of F10 under the same conditions with mixing times of 200 and 500 ms, respectively. Relatively strong NOE's could be observed between the NH's of Gly(14) and Val(15), Val(15) and Arg(16), and Arg(16) and Gly(17). Sequential NH–NH NOE's were also observed between residues Gly(6) and Asp(7), Ala(10) and Glu(11), and Glu(22) and Arg(23). Again, because of overlap of resonances, NOE's could not be identified (too close to the diagonal) between residues Asp(7) and Phe(8), Phe(8) and Leu(9), Leu(9) and Ala(10), Glu(11) and Gly(12), Gly(13) and Gly(14), and Val(20) and Val(21). It is clear that there are no NH–NH NOE's in the region of Asp(2) to Gly(6), Gly(12) and Gly(13), and Arg(19) and Val(20). The extra asymmetric cross-peaks in Figure 5 are due to t_1 noise.

These NOE data are summarized in Table III along with other NMR parameters.

Identification of Long-Range NOE's. We have recorded NOESY spectra of F10 in H_2O with an optimized mixing time (500 ms) at four different temperatures: 25, 5, 0, and −8 °C. No other NOE connectivities could easily be identified between $C^{\alpha}H$ and NH, $C^{\beta}H$ and NH, and NH and NH except for those expected from the short-range i to $i + 1$ amino acid sequence of the peptide. We also recorded NOESY spectra of F10 with optimized mixing times in D_2O at both 5 and 0 °C and in DMSO at 25 °C. Almost all NOE connectivities are explainable in terms of intraresidue and sequential interresidue $C^{\alpha}H$ and $C^{\beta}H$, $C^{\alpha}H$ and $C^{\gamma}H$ interactions.

Binding Studies of F11 with F12. No significant line broadening is present in the resonances of either F11 or F12

when they are mixed at volume ratios from 6:1 to 3:2 (approximate mole ratios of 6:1 to 1:1) of F11:F12. In a previous study, Gly-Pro-Arg-Pro was demonstrated to cause a large degree of line broadening, especially at Ser(3) in F11 in pure water at pH 7.0 (Root–Bernstein & Westall, 1984). Binding experiments at pH 7.0 were more complicated for us. A significant amount of exchange broadening of the NH protons of F11 under our experimental conditions prevented us from using line broadening to assay formation of a peptide complex. Therefore, we can conclude only that no significant binding occurs between the peptide portions Ala(1)–Arg(16) and Gly(17)–Arg(23) at pH 6.0.

Discussion

In Table III, we present a survey of the structurally informative NMR parameters obtained from this study. It is interesting to note that all NH protons exchange very fast within the segment of Ala(1) to Gly(6). Furthermore, the NH chemical shifts in this region are essentially indistinguishable from those of nonstructured peptides in both H_2O and DMSO except for the three residues Asp(2), Ser(3), and Gly(4) which are close to the electron-withdrawing group ^+H_3N–CH-(CH_3)–CO. It is also seen that no strong sequential NOE's exist in this region of the molecule. These NMR observations suggest that this region of the polypeptide backbone is intrinsically flexible; this is compatible with the fact that this region contains highly frequent substitutions when comparisons are made of human fibrinogen and the fibrinogens from other species (Henschen et al., 1983). In contrast, within the relatively conserved region of Asp(7) to Arg(23), we observed relatively slow exchanging NH protons. This sequence also contains residues with altered NH chemical shifts and some strong sequential NOE's. The present NMR data thus provide direct evidence for a previous suggestion (Nagy et al., 1982), based on the immunochemistry of FpA (F11) (Canfield et al., 1976; Wilner et al., 1976, 1979), that the N-terminal region [Ala(1)–Gly(6) in human fibrinogen] is freely accessible and in an unstructured conformation even in the parent fibrinogen molecule, while the region Asp(7)–Arg(16) may be in a specific conformation when attached to the rest of the whole fibrinogen molecule, part of which is the fragment Gly-(17)–Arg(23) present in the peptide F10.

In a previous NMR study of the synthetic peptides encompassing Asp(7) to Val(20), it was observed that the exchange rate of Gly(14) decreases with the addition of distant residues, Asp(7), Arg(19), and Val(20), to the shorter peptide fragment of Phe(8) to Pro(18) (Marsh et al., 1985). In the longer peptide (F10) studied here, *both* the NH of Gly(14) and that of Val(15) exchange slowly with solvent. In fact, the NH exchange rate of Val(15) is even smaller than that of Gly(14) (Figure 4). This can be explained only by the existence of local structure involving the whole segment from Gly(12) to Val-(15). Using conformational energy calculations, we have shown that both sequences (G-G and G-V) have a high probability of formation of a β-bend (Zimmerman & Scheraga, 1978). Recently, it has been reported that the sequence X-G-G-V often exists as a hairpin β-bend in proteins (Sibanda & Thornton, 1985). The NH proton of Val(15) would be hydrogen bonded to the carbonyl of Gly(12) for such a β-bend at residues Gly(13) and Gly(14) [see Figure 4 of Marsh et al. (1983) for a model of this proposed structure]. This hydrogen bond would cause a significantly reduced exchange rate of the NH of Val(15). The existence of this local hairpin structure is further supported by the fact that the NH chemical shift of Val(15) in all of the synthetic peptides from Asp(7) to Val(20), Phe(8) to Pro(18), and Gly(13) to Pro(18) (Marsh et al., 1985) deviates significantly from that of reference peptides in the same manner as in F10 studied here (Table I). Furthermore, the geminal protons of Gly(12) become nonequivalent, and its NH proton is well resolved from the NH protons of other glycines in the sequence, indicating that only a limited number of conformational states are available to this residue (Kessler & Bermel, 1986).

NOE data further support the assignment of the bend structure to residues Gly(13) and Gly(14). Strong sequential $C^\alpha H$–NH and NH–NH NOE's exist between Gly(14) and Val(15) as expected from the proposed β-bend structure discussed above (Wüthrich et al., 1984; Shenderovich et al., 1984; Wagner et al., 1986; Wüthrich, 1986). Unfortunately, the resonances of the $C^\alpha H$ and NH protons of Gly(13) and Gly(14) overlap with each other (Figures 2 and 3 and Table I). The NOE cross-peak designated as G14–V15 in Figure 3 would mask the possible $C^\alpha H(i)$–$NH(i + 2)$ NOE interactions between Gly(13) and Val(15) typically observed for a β-bend (Wagner et al., 1986; Wüthrich, 1986). Furthermore, the interactions between the $C^\alpha H$ of Gly(13) and the NH of Gly(14) and their NH's cannot be identified without ambiguity because of this overlap. Lack of these NOE data makes it impossible to distinguish between different types of β-bends (Wüthrich et al., 1984; Wüthrich, 1986).

In proteins, however, a sequence like X-G-G-V has been found to prefer a type I' β-bend at the two glycines (Sibanda & Thornton, 1985). We thus assume that a type I' β-bend is selectively stabilized and constitutes an essential structural feature in the interaction of thrombin with fibrinogen. This structural element is presumably also responsible for the abnormal temperature coefficients of the NH's of Gly(13) and Gly(14). Specifically, a β-turn would place Glu(11) and Arg(16) in spatial proximity so that the hydrophobic parts of their side chains would interact with those of Val(15). It would even be possible that an ionic interaction such as a salt bridge exists between Glu(11) and Arg(16) which further stabilizes the intervening bend structure. The collective interactions would provide enough of a shielding effect so that the NH chemical shift of Gly(13) and Gly(14) would behave abnormally upon changing the temperature.

The slower exchange rates of the backbone NH protons of Arg(19) and Val(20) suggest that there may be another β-bend structure involving Gly(17) to Val(20), as proposed previously on the basis of NMR studies of small fibrinogen-like peptides (von Dreele et al., 1978). The strong sequential NOE between the $C^\alpha H$ of Pro(18) and the NH of Arg(19) provides further support for the existence of a local structure involving these two residues. However, these NOE data are not sufficient to distinguish between different types of bend structures since we did not observe a strong sequential NH–NH NOE between Arg(19) and Val(20).

Overall, peptide F10 does not assume a compact folded structure (e.g., a rigid β-sheet or α-helix) under the conditions studied, as indicated by the absence of long-range NOE's in both H_2O and DMSO. Presumably, the local backbone structures discussed above are stabilized when the peptide binds to the active site of thrombin. Further experiments, such as transfer NOE studies of an enzyme–substrate complex (Clore & Gronenborn, 1982, 1983), are needed for an understanding of the structural aspects of the specificity of the interaction of thrombin with fibrinogen.

Conclusions

We have completely assigned the resonances of synthetic peptides corresponding to residues 1–23 of the Aα chain of human fibrinogen. Overall, the NMR data suggest the pos-

sible existence of some ordered backbone structure in the region from Asp(7) to Arg(23). NH chemical shifts, NH exchange rates, and strong sequential NOE's suggest that there is a significant population of a β-bend structure around residues Gly(12) to Val(15). This supports a previous proposal that the specificity of the interaction of fibrinogen with thrombin in part lies in a chain reversal that brings the distant Phe(8) close to the Arg(16)–Gly(17) peptide bond. This chain reversal would also bring the negatively charged Asp(7) close to the active site of thrombin when fibrinogen binds to thrombin. Alternatively, Asp(7) might interact directly with Arg(19) within the fibrinogen molecule so that a native structure involving the hairpin bend at Gly(12) to Val(15) is selectively stabilized. Work is in progress on the effects of specific amino acid substitutions (Henchen et al., 1983; Menache, 1983) on the conformational properties within the segment from Asp(7) to Val(20) of the Aα chain of human fibrinogen.

ACKNOWLEDGMENTS

We thank M. Adler, M. A. Delsuc, and G. T. Montelione for helpful discussions. We are indebted to Dr. G. Claeson for a gift of Kabi human fibrinogen and to Dr. J. W. Fenton II for a gift of human α-thrombin.

REFERENCES

Aue, W. P., Bartholdi, E., & Ernst, R. R. (1976) *J. Chem. Phys. 64*, 2229.

Basus, V. J. (1984) *J. Magn. Reson. 60*, 138.

Bax, A., & Drobny, G. (1985) *J. Magn. Reson. 61*, 306.

Billeter, M., Braun, W., & Wüthrich, K. (1982) *J. Mol. Biol. 155*, 321.

Blombäck, B. (1967) in *Blood Clotting Enzymology* (Seegers, W. H., Ed.) pp 143–215, Academic, New York.

Bodenhausen, G., Wagner, G., Rance, M., Sørensen, O. W., Wüthrich, K., & Ernst, R. R. (1984) *J. Magn. Reson. 59*, 542.

Bolton, P. H., & Bodenhausen, G. (1982) *Chem. Phys. Lett. 89*, 139.

Bundi, A., & Wüthrich, K. (1979) *Biopolymers 18*, 285.

Bundi, A., Grathwohl, C., Hochmann, J., Keller, R. M., Wagner, G., & Wüthrich, K. (1975) *J. Magn. Reson. 18*, 191.

Campbell, I. D., Dobson, C. M., & Ratcliffe, R. G. (1977) *J. Magn. Reson. 27*, 455.

Canfield, R. E., Dean, J., Nossel, H. L., Butler, V. P., Jr., & Wilner, G. D. (1976) *Biochemistry 15*, 1203.

Clore, G. M., & Gronenborn, A. M. (1982) *J. Magn. Reson. 48*, 402.

Clore, G. M., & Gronenborn, A. M. (1983) *J. Magn. Reson. 53*, 423.

Dobson, C. M., Lian, L.-Y., Redfield, C., & Topping, K. D. (1986) *J. Magn. Reson. 69*, 201.

Eich, G., Bodenhausen, G., & Ernst, R. R. (1982) *J. Am. Chem. Soc. 104*, 3731.

Englander, S. W., & Poulsen, A. (1969) *Biopolymers 7*, 379.

Hanna, L. S., Scheraga, H. A., Francis, C. W., & Marder, V. J. (1984) *Biochemistry 23*, 4681.

Henschen, A., Southan, C., Kehl, M., & Lottspeich, F. (1981) *Thromb. Haemostasis 46*, 181.

Henschen, A., Lottspeich, F., Kehl, M., & Southan, C. (1983) *Ann. N.Y. Acad. Sci. 408*, 28.

Hogg, D. H., & Blombäck, B. (1978) *Thromb. Res. 12*, 953.

Hore, P. J. (1983) *J. Magn. Reson. 55*, 283.

Hore, P. J. (1984) *J. Magn. Reson. 62*, 561.

Hoult, D. I., & Richards, R. E. (1975) *Proc. R. Soc. London, A 344*, 311.

Jeener, J., Meier, B. H., Bachmann, P., & Ernst, R. R. (1979) *J. Chem. Phys. 71*, 4546.

Kessler, H., & Bermel, W. (1986) in *Methods in Stereochemical Analysis 6: Applications of NMR Spectroscopy to Problems in Stereochemistry and Conformational Analysis* (Takeuchi, Y., & Marchand, A. P., Eds.) VCH, Deerfield Beach.

King, G., & Wright, P. E. (1983) *J. Magn. Reson. 54*, 328.

Laudano, A. P., & Doolittle, R. F. (1980) *Biochemistry 19*, 1013.

Levy, G. C., Delaglio, F., Macur, A., & Begemann, J. (1986) *J. Comput. Enhanced Spectrosc. 3*, 1.

Macura, S., Huang, Y., Suter, D., & Ernst, R. R. (1981) *J. Magn. Reson. 43*, 259.

Marsh, H. C., Jr., Meinwald, Y. C., Lee, S., & Scheraga, H. A. (1982) *Biochemistry 21*, 6167.

Marsh, H. C., Jr., Meinwald, Y. C., Thannhauser, T. W., & Scheraga, H. A. (1983) *Biochemistry 22*, 4170.

Marsh, H. C., Jr., Meinwald, Y. C., Lee, S., Martinelli, R. A., & Scheraga, H. A. (1985) *Biochemistry 24*, 2806.

Meinwald, Y. C., Martinelli, R. A., Van Nispen, J. W., & Scheraga, H. A. (1980) *Biochemistry 19*, 3820.

Menache, D. (1983) *Ann. N.Y. Acad. Sci. 408*, 121.

Molday, R. S., Englander, S. W., & Kallen, R. G. (1972) *Biochemistry 11*, 150.

Montelione, G. T., Wüthrich, K., Nice, E. C., Burgess, A. W., & Scheraga, H. A. (1987) *Proc. Natl. Acad. Sci. U.S.A. 84*, 5226.

Morris, S., Denninger, M. H., Finlayson, J. S., & Menache, D. (1981) *Thromb. Haemostasis 46*, 104.

Nagy, J. A., Meinwald, Y. C., & Scheraga, H. A. (1982) *Biochemistry 21*, 1794.

Piatini, U., Sørensen, O. W., & Ernst, R. R. (1982) *J. Am. Chem. Soc. 104*, 6800.

Plateau, P., & Guêron, M. (1982) *J. Am. Chem. Soc. 104*, 7310.

Rae, I. D., & Scheraga, H. A. (1979) *Int. J. Pept. Protein Res. 13*, 304.

Root-Bernstein, R. S., & Westall, F. C. (1984) *Proc. Natl. Acad. Sci. U.S.A. 81*, 4339.

Sarin, V. K., Kent, S. B. H., Tam, J. P., & Merrifield, R. B. (1981) *Anal. Biochem. 117*, 147.

Scheraga, H. A. (1983) *Ann. N.Y. Acad. Sci. 408*, 330.

Scheraga, H. A. (1986) *Ann. N.Y. Acad. Sci. 485*, 124.

Shaka, A. J., & Freeman, R. (1983) *J. Magn. Reson. 51*, 169.

Shenderovich, M. D., Nikiforovich, G. V., & Chipens, G. I. (1984) *J. Magn. Reson. 59*, 1.

Sibanda, B. L., & Thornton, J. M. (1985) *Nature (London) 316*, 170.

States, D. J., Haberkorn, R. A., & Ruben, D. J. (1982) *J. Magn. Reson. 48*, 286.

Takeda, M., & Stejskal, E. O. (1960) *J. Am. Chem. Soc. 82*, 25.

Telford, J. N., Nagy, J. A., Hatcher, P. A., & Scheraga, H. A. (1980) *Proc. Natl. Acad. Sci. U.S.A. 77*, 2372.

Von Dreele, P. H., Rae, I. D., & Scheraga, H. A. (1978) *Biochemistry 17*, 956.

Wagner, G. (1983) *J. Magn. Reson. 55*, 151.

Wagner, G., & Wüthrich, K. (1982) *J. Mol. Biol. 155*, 347.
Wagner, G., Neuhaus, D., Wörgötter, E., Vasak, M., Kagi, J. H. R., & Wüthrich, K. (1986) *J. Mol. Biol. 187*, 131.
Wider, G., Lee, K. H., & Wüthrich, K. (1982) *J. Mol. Biol. 155*, 367.
Wider, G., Macura, S., Kumar, A., Ernst, R. R., & Wüthrich, K. (1984) *J. Magn. Reson. 56*, 207.
Wilner, G. D., Nossel, H. L., Canfield, R. E., & Butler, V. P., Jr. (1976) *Biochemistry 15*, 1209.
Wilner, G. D., Thomas, D. W., Nossel, H. L., Robbins, P. F., & Mudd, M. S. (1979) *Biochemistry 18*, 5078.
Wüthrich, K. (1986) *NMR of Proteins and Nucleic Acids*, Wiley, New York.
Wüthrich, K., Wider, G., Wagner, G., & Braun, W. (1982) *J. Mol. Biol. 155*, 311.
Wüthrich, K., Billeter, M., & Braun, W. (1984) *J. Mol. Biol. 180*, 715.
Zimmerman, S. S., & Scheraga, H. A. (1978) *Biopolymers 17*, 1871.
Zuiderweg, E. R. P. (1987) *J. Magn. Reson. 71*, 283.

Lipid–Lipid Interactions in Reconstituted High-Density Lipoproteins by Deuterium Nuclear Magnetic Resonance†

David B. Fenske, Yashpal I. Parmar,‡ W. Dale Treleaven, Ravinder S. Chana, and Robert J. Cushley*
Department of Chemistry, Simon Fraser University, Burnaby, British Columbia, Canada V5A 1S6
Received April 24, 1987; Revised Manuscript Received February 4, 1988

ABSTRACT: Lipid–lipid interactions between the core and monolayer have been studied by using reconstituted high-density lipoproteins (rHDLs) composed of apoHDL$_3$ with either dipalmitoylphosphatidylcholine (DPPC) or egg phosphatidylcholine (egg PC) as the monolayer and either cholesteryl oleate (CO) or triolein (TO) as the core. The effect of the monolayer on the core was observed by deuterium nuclear magnetic resonance (^{2}H NMR) studies of rHDLs containing the core component cholesteryl [18,18,18-$^2H_3$]oleate ([$^2H_3$]CO) or tri[16,16-$^2H_2$]oleoylglycerol ([$^2H_6$]TO) surrounded by a monolayer of either DPPC or egg PC as a function of temperature. The reverse effect, that of the core on the monolayer, was examined by both ^{2}H and ^{31}P NMR studies of rHDLs containing [5,5-$^2H_2$]PC in the presence of CO or TO as a function of temperature. The ^{2}H NMR line widths of [$^2H_3$]CO and [$^2H_6$]TO were considerably broader and showed a greater temperature dependence in rHDLs containing DPPC than in those containing egg PC. Similarly, the C–^{2}H order parameters of [$^2H_2$]PC were higher and showed a greater temperature dependence in rHDLs containing CO than in those containing TO. In contrast, the ^{31}P NMR line widths were identical for both [$^2H_2$]-PC/CO/apoHDL$_3$ and [$^2H_2$]PC/TO/apoHDL$_3$ at 25 and 6 °C, showing only a slight temperature dependence. Thus, acyl chains of both the monolayer and core components show increased order when in contact with neighboring lipids of higher order. The data demonstrate a direct effect of core cholesteryl esters and triglycerides with the phospholipid monolayer of HDL.

Human plasma high-density lipoproteins (HDLs)[1] play an important role in both lipid transport and cholesterol homeostasis in the circulatory system (Scanu, 1979). Plasma HDL concentrations have been inversely correlated with the risk of ischemic heart disease (Miller & Miller, 1975). This antiatherogenic effect is thought to involve cholesterol efflux from the peripheral tissues (Tall & Small, 1979). The mechanism, known as reverse cholesterol transport, may proceed via esterification of HDL cholesterol by the enzyme lecithin:cholesterol acyltransferase (Tall & Small, 1979). The cholesteryl esters so produced may then be transported to the liver via HDL or transferred to the other lipoproteins by the action of lipid transfer proteins present in the plasma (Zilversmit, 1984).

The structural organization of HDLs must determine their biological roles, and thus the structure and dynamics of the lipid constituents are of considerable interest. Many techniques have been used to probe HDL structure, including electron microscopy (Forte et al., 1968), X-ray diffraction (Laggner & Muller, 1978; Baumstark et al., 1983), ESR (Brainard et al., 1980), and NMR (Finer et al., 1975; Henderson et al., 1975; Hamilton et al., 1974; Hamilton & Cordes, 1978; Wassall et al., 1982; Parmar et al., 1983). A widely accepted model of HDL structure is that of a quasi-spherical particle of 6.5–12-nm diameter (Forte et al., 1968; Scanu, 1979; Laggner & Muller, 1978) with protein, phospholipid, and cholesterol in an outer monolayer and cholesteryl esters and triglyceride in a hydrophobic core (Smith et al., 1978). There is considerable debate, however, regarding the organization

† This work was supported by the British Columbia Heart Foundation.
* Author to whom correspondence should be addressed.
‡ Present address: Shaughnessy Hospital Research Center, University of British Columbia, 950 West 28th Ave., Vancouver, British Columbia, Canada V5Z 4H4.

[1] Abbreviations: rHDL, reconstituted high-density lipoprotein; ^{2}H NMR, deuterium nuclear magnetic resonance; ^{31}P NMR, phosphorus-31 nuclear magnetic resonance; DSC, differential scanning calorimetry; [$^2H_3$]CO, cholesteryl [18,18,18-$^2H_3$]oleate; [$^2H_2$]PC, phosphatidylcholine synthesized from egg L-α-lysophosphatidylcholine and [5,5-$^2H_2$]palmitic acid; [$^2H_{31}$]PC, phosphatidylcholine synthesized from egg L-α-lysophosphatidylcholine and [$^2H_{31}$]palmitic acid; [$^2H_6$]TO, tri[16,16-$^2H_2$]-oleoylglycerol; egg PC, egg phosphatidylcholine; DPPC, dipalmitoylphosphatidylcholine; TO, triolein; CO, cholesteryl oleate; apoHDL$_3$, apoproteins isolated from HDL$_3$; ESR, electron spin resonance; TLC, thin-layer chromatography; SDS, sodium dodecyl sulfate.

0006-2960/88/0427-4491$01.50/0